THE JOURNAL OF PHYSICAL CHEMISTRY A

Article

pubs.acs.org/JPCA

The Dimerization of H_2NO

Peng Xu and Roald Hoffmann*

Department of Chemistry and Chemical Biology, Baker Laboratory, Cornell University, Ithaca, New York 14853-1301, United States

Supporting Information

ABSTRACT: H_2NO is the prototype of aminoxyls, kinetically persistent free radicals. The potential dimerization and reaction modes of H_2NO are examined. The dimer potential energy surface features a barely metastable O−O bound species and several locally bound dimeric structures. One of these, a rectangular or rhomboid O−N−O-N ring, is a characteristic structural feature of more stable aminoxyls in the solid state. Its electronic structure is related to other four-center six-electron systems. A general picture of the weak dimer binding is constructed for these and other H_2NO dimers from a balance of four-electron repulsions between NO π electrons, and two-electron attractive interaction between the singly occupied π^* orbitals of the diradical. The most stable diradical structure is a surprisingly strongly hydrogen bonded dimer diradical. The barriers separating the other isomers from this global minimum are calculated to be small.

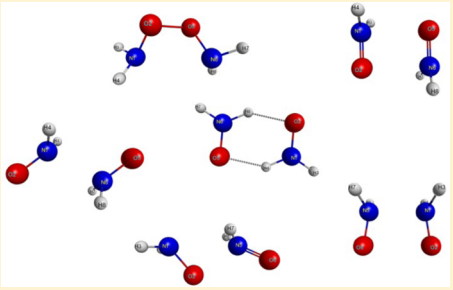

1. INTRODUCTION

Aminoxyl radicals, R_2NO, form a family of odd-electron species involved in many reactions.[1,2] Depending on the R groups, the persistence of R_2NO radicals under ambient conditions varies; many are isolable as pure compounds, yet others are only fleeting, observed spectroscopically. Due to their relative stability, aminoxyl radicals have been employed widely as electron spin resonance (ESR) probes, as well as spin labels or spin traps in studying biochemical processes,[3,4] and in polymer chemistry.[5] Molecular-based magnets using aminoxyl radicals as building blocks have also been explored.[6]

According to the IUPAC gold book,[7] $R_2NO\bullet$ radicals should be named as aminoxyls, for their relation to hydroxylamine. In common usage they have also been called "nitroxides" and "nitroxyl radicals".[8] These terms are, however, potentially confusing, as they might suggest the presence of a nitro group. And the nitroxyl label has also been used for HNO. In this paper we use the IUPAC name, aminoxyl.

The impetus for our study came from a desire to design aminoxyl diradicals with an intermediate level of radical interaction. This led us to look in general at the stability, thermodynamic and kinetic, of aminoxyls. That in turn led us to examine their reaction modes. We begin here with the simplest of these, H_2NO.

Chemical experience tells us that the common fate of radicals is dimerization (or polymerization) with low activation energy, if not barrierless, and atom abstraction, or addition to a double bond, where those reaction channels are possible. Then what makes a stable/persistent radical persist in its free form? In general, increasing steric encumberment near the radical centers enhances persistence. The simplest aminoxyl H_2NO, having no such protection, is highly reactive, and can only be detected spectroscopically, whereas $CH_3(H)NO$ is already more stable than H_2NO.[9]

Though low activation reaction channels are available to some higher aminoxyls (for instance those with α hydrogens), the reaction that appears to be most common for radicals, namely dimerization, does not appear to be observed. We wanted to see the reasons for this, and took the archetype H_2NO as a model.

The H_2NO radical has been detected in the gas phase by far-infrared laser magnetic resonance spectroscopy,[10] in solution[2,11,12] and in a xenon matrix[13] by ESR. The microwave rotational spectrum of H_2NO in the gas phase has also been studied.[14] These studies suggested that the ground-state structure of H_2NO is essentially planar (C_{2v}), although the possibility of a double minimum potential with a low barrier for pyrimidalization at the nitrogen cannot be excluded.

On the theoretical side, studies of the parent aminoxyl date back to 1970, their focus being the equilibrium structure and hyperfine coupling constant of the free radical.[15−26] There has been much back and forth on whether H_2NO is planar or pyramidal, with conclusions sensitive to the level of theory and basis sets. Barone et al. predicted a pyramidal double minimum with a < 1 kcal/mol inversion barrier.[17] Pauzat, Gritli, Ellinger and Subra studied the vibrational structure of H_2NO; their key finding is that the first out-of-plane vibrational level lies above the inversion barrier.[20] This has been confirmed by Haring et al.[21] and Komaromi and Tronchet.[24] The question of the planarity of H_2NO then becomes somewhat of an "academic" one.

There is broad astrochemical interest in stable and metastable species in the interstellar medium. Ulich, Hollis, and Snyder detected HNO in the interstellar clouds Sgr B2 and NGC 2024.[27,28] Nitric oxide (NO) has also been detected in

Received: December 28, 2015
Revised: February 3, 2016
Published: February 4, 2016

DOI: 10.1021/acs.jpca.5b12674
J. Phys. Chem. A 2016, 120, 1283−1296

Sgr B2[29] and later in the dark cloud L134N.[30] A third NO containing molecule, nitrous oxide (N_2O), was observed toward Sgr B2(M).[31] Although H_2NO has not yet been detected in interstellar clouds, its existence in the cold environment of the interstellar medium has been implicated.[14]

There is yet another reason to be interested in H_2NO. Ammonia (NH_3) released into the atmosphere decomposes to NH_2 radical, either by direct photolysis or attack by OH radicals in the troposphere. $\bullet NH_2$ (like $\bullet$Cl and $\bullet$OH) can initiate a catalytic cycle for the decomposition of ozone, O_3, in the atmosphere,[32] in which aminoxyl is an intermediate:

$$NH_2 + O_3 \rightarrow H_2NO + O_2$$
$$H_2NO + O_3 \rightarrow NH_2 + 2O_2 \quad (1)$$

These reactions have been studied both theoretically and experimentally.[33−38]

The aim of our work is to gain an understanding of the dimerization of H_2NO, so as to be able to think about stabilizing electronically higher aminoxyls, R_2NO, and diradicals based on these. To the best of our knowledge, the potential energy surface (PES) of the dimers of H_2NO has not been explored in detail. There is one computational study on the H_2NO dimer, by Saito et al.,[39] which focused on the magnetic interaction of two H_2NO molecules in a fixed geometry. Our detailed study of the dimer PES will complement our understanding of the role H_2NO might play in both astrochemistry and atmospheric chemistry, and add to our knowledge of the chemistry of more complicated aminoxyls.

2. RESULTS AND DISCUSSION

2.1. H_2NO Monomer. Before we dive into the reasonably complicated H_2NO dimer PES, let us first examine the structure of the monomeric H_2NO radical, widely calculated by others. We calculated the H_2NO monomer at the B3LYP/cc-pVTZ, MP2/cc-pVTZ, and MRMP/cc-pVTZ levels of theory. These methods are described in the Computational Methodology section at the end of this paper. The geometrical parameters of our calculations agree reasonably well with experimental results (Table 1). The latter are consistent with an essentially planar structure, but note the substantial disagreement between the experimental values for the NO distance. We tend to believe the shorter (1.28 Å) value is more accurate.

Table 1. Geometrical Parameters of H_2NO Computed by Various Levels of Theory and from Experiments

	N−O distance (Å)	N−H distance (Å)	H−N−H angle (deg)	out of plane angle (deg)
B3LYP[a]	1.27	1.02	118	21
UMP2[a]	1.26	1.01	119.5	0
MRPT(1,1)[a]	1.25	1.01	119	0
exp[10]	1.34	0.99	122	0
exp[14]	1.28	1.01	123	0

[a]The cc-pVTZ basis set is used.

2.2. General Aspects of the Electronic Structure of H_2NO. For aminoxyls, one generally writes resonance structures **1** and **2** in Scheme 1. This would also be true for H_2NO.

The unpaired electron is placed on the oxygen in **1**, on the nitrogen in **2**. This immediately broaches the question bothering both theorists and experimentalists: What is the distribution of that radical electron among N and O? In valence bond language this could simplistically be rephrased as a question of the relative contribution to the wave function of resonance structure **1** and **2**.

Scheme 1. Two Resonance Structures for R_2NO

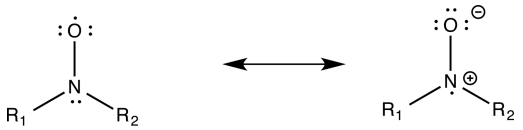

1 **2**

In simple molecular orbital terms, R_2NO has one electron more than R_2CO, a ketone, i.e., the radical enters an orbital like the π^* MO of a ketone. The immediate implication is a π-radical, and a rough distribution of the unpaired electron over both N and O. Figure 1 shows one contour of the singly occupied π^* molecular orbital (SOMO) of aminoxyl from an second-order perturbation level calculation. Qualitatively, one might expect more of unpaired electron density on N than O, as there is a general perturbation-theory-based regularity that, if an MO is formed from component AOs of atoms of different electronegativity, the bonding (here π) combination is more localized on the more electronegative atom, but the antibonding orbital (π^*) is more localized on the less electronegative one (here N).[40]

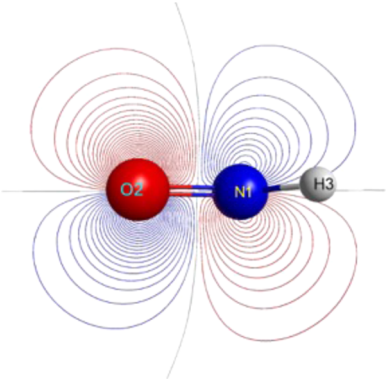

Figure 1. Contours of the singly occupied π^* molecular orbital (SOMO) of aminoxyl with contour value of $\psi = 1.0$. The view is in the molecular plane.

The spin density can be measured by polarized neutron diffraction (PND), as well as by other techniques such as NMR and EPR. To the best of our knowledge, there has not been an experimental determination of the spin distribution in H_2NO itself. The more complex aminoxyl diradical $C_8H_{12}O_4((CH_3)_4C_5H_5NO)_2$, tanol suberate, was the first radical studied by PND.[41] Since the two NO groups in the same diradical are separated by at least 6 Å, each NO group is considered isolated. The PND result revealed an approximately equal distribution of spin between N and O atoms. In another study, Bordeaux et al. determined, by PND, the spin density of 4-oxo-2,2,6,6-tetramethyl-1-piperidinyloxy (tempone) to be roughly equal on N and O atoms and the spin density of 4-hydroxy-2,2,6,6-tetramethyl-1-piperidinyloxy (tempol) to be ~54% on the N center.[42] These experimental results are qualitatively compatible with our simple MO picture, where the unpaired π^* electron is somewhat more localized on N.

DOI: 10.1021/acs.jpca.5b12674
J. Phys. Chem. A 2016, 120, 1283−1296

Theory has struggled to predict the spin partitioning between N and O. UHF calculations on a series of radicals from H_2NO to $C_5H_{10}NO$ showed spin transfer from O to N as R groups get larger, with only 22% spin density on N for H_2NO.[43] This trend was observed with other theoretical approaches as well.[44,45] Yet even $C_5H_{10}NO$ has a distribution of 35%/65% spin density on N and O at UHF level.[43,46] One might wonder about the geometry of H_2NO used in those studies, but it turned out that the spin density was not greatly influenced by geometry.[45] Spin populations calculated by iterative CI with a 6-31G** basis set gave ~0.38/0.64 N/O spin distribution.[45] In the same study, the authors pointed out the importance of basis-set quality and electron correlation in determining spin population in aminoxyls.

We calculated Mulliken spin populations with unrestricted Møller–Plesset second-order perturbation theory (UMP2), and compared the values obtained with various other levels of theory in Table 2 below. Unfortunately the program we use currently does not allow spin population calculation at the multireference perturbation level of theory. We see from Table 2 that at the Hartree–Fock (HF) level, the spin density is quite localized on oxygen. The restricted and unrestricted DFT (B3LYP) methods yield a similar spin distribution, with some spin density shifting from O to N. The DFT results compare well with a previous iterative CI calculation using a different basis set.[45] Finally, UMP2 calculations yield a much more evenly distributed spin density between N and O. Nevertheless, the unpaired electron resides more on O than N, in disagreement with the simplest polarization argument for the makeup of the π^* orbital.

Table 2. Mulliken Spin Population by Unrestricted (U) or Restricted (RO) Methods: MP2 and B3LYP[a]

	UMP2	UHF	UB3LYP	ROB3LYP
N	0.495	0.312	0.401	0.382
O	0.538	0.733	0.613	0.595
H	−0.017	−0.022	−0.007	0.011
H	−0.017	−0.022	−0.007	0.011

[a]The basis set used is cc-pVTZ.

2.3. An Isomer, HNOH. For comparison, we optimized the geometry of a constitutional isomer of H_2NO, HNOH, more specifically, *trans*-HNOH, which is the photoproduct of excited NO in solid H_2 with vacuum-ultraviolet radiation.[47] Note that we only calculated the *trans*-form of HNOH; the *cis*-form is computed to be less stable than the *trans*-form by about 4.8 kcal/mol, presumably due to repulsion between lone pairs on N and O.

HNOH is planar. At the same level of theory, the NO bond length in HNOH is longer (1.36 Å) than that in H_2NO (1.25 Å). The HNOH radical is ~8.7 kcal/mol less stable than H_2NO. HNOH, of course, is also a radical, with its unpaired electron in a π^* orbital across N–O. This isomer has one electron more than diazine, HN=NH, and one electron less than (nonplanar) hydrogen peroxide, HOOH. In contrast to H_2NO, we see in HNOH the expected electron density distribution based on the electronegativity-perturbation argument given earlier (Figure 2).

The relative instability of HNOH and the electron distribution of its SOMO may be related to the two resonance forms one can draw for an HNOH radical (Scheme 2), as for H_2NO, each placing the radical electron on different centers.

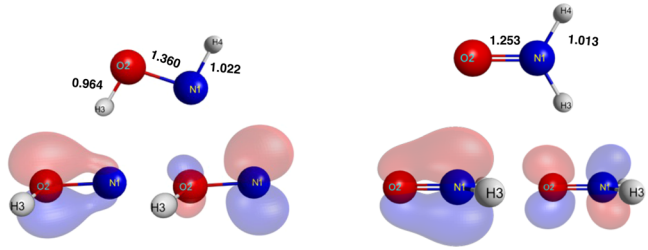

Figure 2. Geometric parameters as well as the π and π^* orbitals of HNOH (left) and H_2NO (right). Note that the atom H4 is hidden in the orbital views.

Scheme 2. Two Resonance Structures for *trans*-HNOH

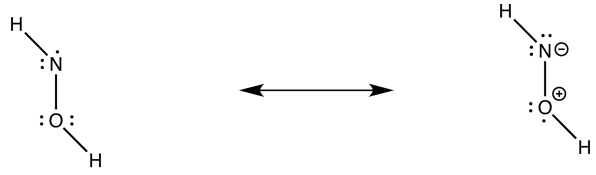

3 4

The charge-separated resonance structure **4** has formal positive and negative charges on O and N, respectively, the opposite of what one expects based on the electronegativity of those elements. One would not expect the valence bond (VB) structure **4** to contribute much, and this is in accord with relative stability and the electron distribution in its SOMO.

2.4. Lewis Structures, and Perceived Impediments to Dimerization of H_2NO. The general perception of the community is that dimerization of "stable" free radicals might be inhibited by the steric bulk of their substituents, by delocalization of the radical spin, and/or the instability of the dimers. For H_2NO, the first disincentive to dimerization is absent, and one is naturally led to think of dimer instability connected to stabilizing delocalization in the monomer.

The dimers that first come to mind are **5**, **6**, and **7** (see Scheme 3), the outcomes of O–O, N–N, and N–O bond formation. In such processes a new bond (likely to be weak) is formed, and any special stabilization of the radical NO bond is lost. The latter stabilization has been variously called the delocalization or resonance energy of the aminoxyl. By a careful thermochemical argument, Rozantsev in his pioneering work[48]

Scheme 3. Five Lewis Structures of $(H_2NO)_2$[a]

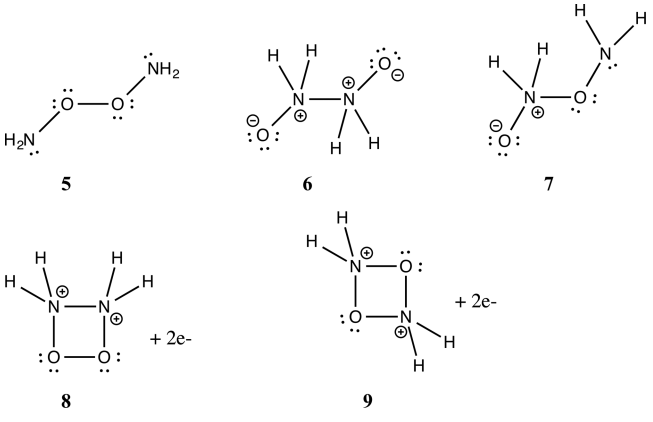

5 6 7 8 9

[a]The untypical notation for structures **8** and **9** is explained in the text.

DOI: 10.1021/acs.jpca.5b12674
J. Phys. Chem. A 2016, 120, 1283–1296

estimated the NO bond strength in aminoxyls at ∼100 kcal/mol, in-between the bond strengths of NO single and double bonds. He estimated the delocalization energy of the aminoxyl bond to be ∼30 kcal/mol, and while the underlying H_2NO-H bond energies have been reexamined in detail,[49,50] this value has remained a reasonable one. The net result is that the loss in stabilization of two aminoxyls, ∼ 60 kcal/mol, is greater in magnitude than the stabilization gained in forming any O−O, N−N, or N−O bond in the dimers.[51,52]

The special stability afforded to the monomer by two-center three-electron bonding has been also addressed by Linnett[53,54] and Harcourt.[55]

The thermochemical argument is convincing, but we suspected there was more to the story of interacting aminoxyls. This is the reason we explore the H_2NO dimer potential energy surface in some detail.

Some electronic structure considerations external to this paper led us also to consider cyclic dimers **8** and **9** in Scheme 3. The Lewis structure formalism has real troubles with the cyclic "head-to-head" (**8**) and "head-to-tail" (**9**) dimers—in these the two "extra" electrons enter a σ^* orbital of the ring. There are, however, good reasons (to which we will return) to think of these as possibilities, for they are analogous, in their bonding, to cyclic iso(valence)electronic S_4^{2-}, cyclobutane dianion, and tetracyanoethylene anion dimers. We will return to this analogy below.

2.5. The Complex $(H_2NO)_2$ Dimer Surface. The full potential energy surface for the dimers of H_2NO is not simple, and, maybe to some extent, dependent to some extent on the level of the calculation. (See SI section I)

On the MRMP surface, we have located 6 local minima, as shown in Figure 3, with their energies relative to separated monomers shown below the figures.

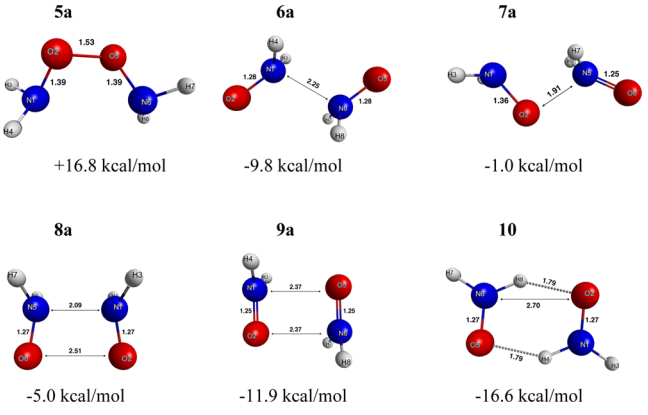

Figure 3. MRMP minimum energy structures. Selected distances are indicated on the graphs in units of Å, the energy relative to two separated monomers is shown below the graphs.

Lewis structure **5**, the O−O bonded dimer, is represented by one local minimum, **5a**, at high energy, but with no imaginary frequencies. The calculated O−O bond length in **5a** is 1.53 Å; a comparison might be to hydrogen peroxide or R—O−O—R, with O−O 1.47 Å.[56] So the O−O bond in **5a** is pretty much fully formed, even if it appears elongated. Note also the elongation of the NO bond, by more than 0.1 Å from the monomer aminoxyl, fully in accord with Lewis structure **5**. The N−O−O−N dihedral angle in **5a** is 69°.

To anticipate a point that will be discussed below, while structure **5a** is a local minimum, it is barely so. There is in our calculation only a tiny barrier to **5a** rearranging to another isomer, **8a**.

Local minimum **6a** resembles the N−N bonded Lewis structure **6**. The NN separation, 2.15 Å, is, however, very long; in comparison, the N−N single bond in hydrazine, H_2NNH_2, is 1.45 Å.[57] Also, the NO bond length is pretty much unchanged from that in the monomer radical. Even if the NN bonding is weak, the −10 kcal/mol energy relative to separated monomers indicates some bonding interaction between the aminoxyl moieties. The ONNO atoms of **6a** are in one plane (i.e., O−N—N−O dihedral angle = 180°) and the hydrogens stay symmetric about this plane. The potential energy surface around **6a** is quite flat; our computations point to a very similar local minimum energy structure of almost the same binding energy, call it **6b** (not shown in Figure 3). In **6b**, one oxygen atom is off the plane formed by the other three heavy atoms (O−N—N−O dihedral angle =145°). Similar but distinct local minima, a sign of a shallow potential energy surface, are not a surprising result for these weakly bound dimers.

Dimer **7a** resembles Lewis structure **7**. The O−N separation between the two aminoxyls is 1.91 Å. Hydroxylamine has an N−O bond length of 1.45 Å,[58] so the NO separation in **7a** indicates weak bonding interaction, in agreement with the slight negative stabilization energy. Interestingly, one of the NO distances, the one corresponding to the N-oxide in valence structure **7**, is unchanged from the monomer; the other NO bond is elongated.

In terms of closeness of the newly formed bond to a covalent single bond length, dimer **5a** structure essentially forms a full bond, followed by dimer **7a** and last dimer **6a**. Interestingly, stability-wise (binding energy relative to monomers), the order is reversed.

Next let us examine the "head-to-head" cyclic dimer **8a** and its "head-to-tail" counterpart, **9a**. In these, the intraradical NO distance is short, but there are long, weakly bonding contacts to the partner radical. The N−N (2.09 Å) and O−O distances (2.51 Å) are quite different in dimer **8a**, but the two intermolecular N−O distances (2.37 Å) are the same in dimer **9a**.

Upon dimerization, pyramidalization at N occurs for both dimer **8a** and dimer **9a**. There are many ways to define pyramidalization in substituted three-coordinate centers; we choose the angle the N−O bond makes with the plane formed by H−N—H, β, as a measure (see SI section II for definition). β in **8a** is 29°, but less for dimer **9a**, with β = 18°, as the structures in Figure 2 suggest. Also notice that the direction of pyramidalization at N is different in these two structures: in **8a**, NH_2 units are pointing "away" from each other, whereas the H's of **9a** are actually slightly shifted toward the O atoms.

Let us try to understand these dimer geometries, as weak as the interactions are. Dimers **8a** and **9a** are cyclic, and iso(valence)electronic with the Jahn−Teller distorted, rectangular S_4^{2-} structure.[59−61] The iso(valence)electronic sequence is $S_4^{2-} \rightarrow O_4^{2-} \rightarrow (HNO)_2^{2-} \rightarrow (H_2NO)_2$. The initial expectation is that both dimers might exhibit similar rectangular distortions. The "starting point", a hypothetical cyclic $(H_2NO)_2^{2+}$ dication, not Jahn−Teller distorted, should have about equal distances in the two ring isomers, as a typical O−O distance is 1.47 Å,[56] an N−N one is 1.45 Å,[57] and N−O is 1.45 Å,[58] all pretty much the same. Adding two electrons to reach the neutral, one comes to a hypothetical cyclic "square"

DOI: 10.1021/acs.jpca.5b12674
J. Phys. Chem. A 2016, 120, 1283−1296

structure $(H_2NO)_2$. This is now very unstable, ~ 184 kcal/mol higher than separated monomer in a single point calculation. One might expect rectangular distortions in the second-order Jahn−Teller distorted neutral ring dimer (second order, as the degeneracies of S_4^{2-} or cyclobutane dianion are no longer there). We see that in the "head-to-tail" **9a**, but an unusual, different, trapezoidal distortion occurs in the "head-to-head" dimer **8a**. In the SI we examine the reasons for the very different geometries of the dimers.

There is also an analogy here to the bonding in the dimers of $TCNE^-$,[62−64] and a variety of examples of "pancake bonding".[65] This connection will be explored elsewhere.

Dimer **9a** is substantially stabilized, −12 kcal/mol below two monomers. And here we have some indirect experimental evidence that this structure is real. Such dimeric entities, featuring intermolecular interactions, have been observed experimentally for some, hardly all, larger aminoxyl radicals in the solid state.[66−68] Figure 4 shows a selection of three

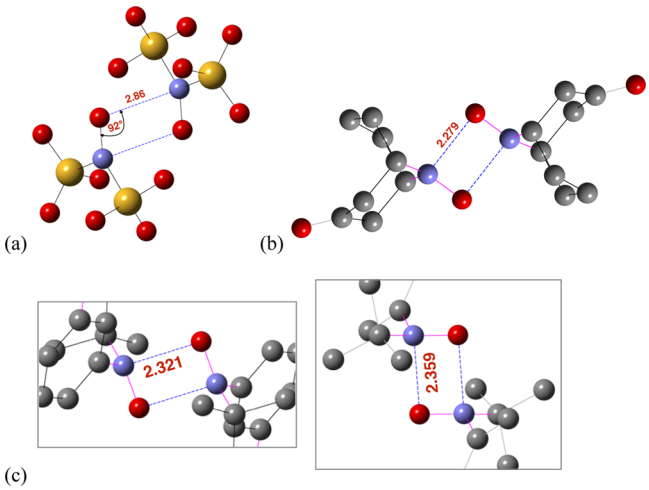

Figure 4. Selected crystal structures of larger aminoxyls that have been found to adopt a dimer structure resembling **9a** in the solid state. (a) triclinic Fremy's salt, (b) CYNOAZ10, and (c) AZOMAD structures (CSD structure notation). The oxygen (red), nitrogen (blue), yellow (sulfur), and gray (carbon) are represented as spheres. For structure a, potassium ions are omitted for clarity. For structures b and c, several atoms are omitted in order to show the rectangular inner $(R_2NO)_2$ region of the dimer structure more clearly. Their full structures are given in the SI. The short NO distance in all cases is 1.25−1.30 Å.

structures; 14 more may be found in Cambridge Structure Database (CSD).[69−71] The N···O distances in the known crystal structures range between 2.27 and 2.86 Å. Note the distinct rectangular arrangement in the segment of the three structures shown.[72] Given the many steric factors and crystal packing adjustments that of necessity intervene for these larger molecules, we think the weak dimerization of two H_2NO molecules in the mode of dimer **9a** is supported by these structures of more complex aminoxyls.

We also looked for the lowest triplet state of these dimers; it turned out that all of them optimized into the triplet state of the global singlet minimum we are about to discuss. If one followed the trajectories of all triplets in the course of optimization, they first went through a separation phase, and then redimerized.

We might mention here that while OO-bonded aminoxyl dimers (for R ≠ H) are not known, such molecules have been synthesized for the corresponding SS-bonded R_2NS radicals.[73−75] Tao Zeng has pointed out to us that this is consistent with resonance structure **2** (the S equivalent) being less important, for electronegativity reasons for R_2NS.

2.6. A Hydrogen-Bonded Dimer. The surprise in our exploration of the (H_2NO) surface was dimer **10** on the singlet surface, the most stable (with our MRMP method) of the dimers. It is clearly a nice, symmetrically hydrogen-bonded aggregate of two aminoxyls. In all the other minima, stabilization is achieved, with varying success, from the overlap and interaction of the diradical orbitals that bear the spin. However, in **10** the singly occupied molecular orbital (SOMO) interaction is minimized, because the SOMO π^* orbitals are arranged in a "side-by-side" parallel fashion, while the NO moieties are 2.7 Å apart. Figure 5 shows the nearly degenerate in- and out-of-phase combinations of the two singly filled orbitals in this structure; their lack of overlap is evident.

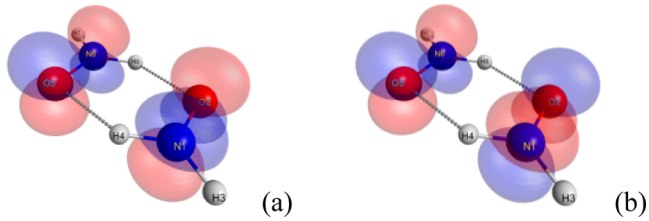

Figure 5. Nearly degenerate in- and out of phase combinations of the two singly occupied orbitals of dimer **10**.

A mark of the lack of interaction of the radical centers in **10** may be seen in the near degeneracy in energy of the lowest singlet and triplet arising. The two are just 0.02 eV apart.

Dimer **10**, as stable as it seems on this surface, is likely only a candidate for matrix isolation. However, a CSD search came up with some fascinating related structures in the literature. One is a molybdenum-coordinated complex with an $(H_2NO)_2$ hydrogen-bonded motif similar to **10** (Figure 6).[76] This Mo complex is the first structurally characterized 7-coordinated complex

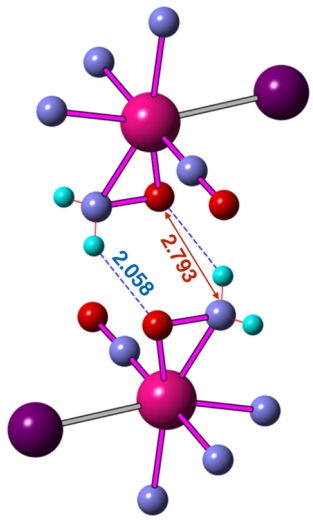

Figure 6. A part of the crystal structure of a Mo-coordinated H_2NO complex, featuring a dimer **10**-like structure. The oxygen (red), nitrogen (light blue), and hydrogen (cyan), molybdenum (magenta), iodine (purple) atoms are represented as spheres. The carbon atoms have been omitted for clarity. The full structure is in the SI.

DOI: 10.1021/acs.jpca.5b12674
J. Phys. Chem. A 2016, 120, 1283−1296

based on the {Mo(NO) (Tp^{Me2})} ([Tp^{Me2}]$^-$ = hydrotris(3,5-dimethylpyrazol-1-yl)borate). Just like dimer **10**, it possesses a center of symmetry. In this complex, H_2NO is a ligand coordinated to Mo. Upon coordination, the molecular N−O bond length is elongated to ∼1.39 Å, compared to that of isolated H_2NO (1.25 Å).

How should we think of H_2NO in this organometallic complex? First, imagining it is neutral H_2NO, it seems quite remarkable to have it stabilized. But then that is the magic (quite understandable magic) of organometallics: ML_n fragments (M = transition metal atom) can stabilize molecular structures that by themselves have minimal kinetic persistence. Examples are CR, CR_2, CCR_2, $C(CH_2)_3$, etc.

The debate on whether the ligands are to be viewed as Lewis bases, charged as need be (e.g., CH_3^-), or as neutral, continues. Are ethylene complexes such, or are they metallacyclopropanes? The answer is "both", but with definite stereochemical signatures of each extreme mode of bonding. In the context of H_2NO as a ligand, one could consider it a two-electron H_2NO^+, π-bonding like an olefin, or a three-electron H_2NO, or a four-electron H_2NO^-, like peroxide. The NO bond elongation is certainly consistent with further population of NO π^* (or depopulation of π). A calculation of H_2NO^- give N−O 1.44 Å, and the pyramidalization at N goes along with coordination.

However, let us focus not on the Mo−H_2NO bonding, but on the interaction between H_2NOs in different molecules. Note how the (coordinated) H_2NO dimer looks like **10**. The hydrogen bonding H···O distance is ∼2.06 Å, with reservations on the reliability of crystallographically determined distances to H, which is longer than that in dimer **10**; the intermolecular N···O distance in this metal complex crystal is ∼2.79 Å, similar to our calculated value in $(H_2NO)_2$. Although this hydrogen-bonded form of the Mo−H_2NO complex is stable in the solid phase, it appears to be unstable at room temperature in solution.[76]

A CSD search also reveals a few $(RHNO)_2$ structures that form such hydrogen-bonded structures, all coordination compounds with a metal center; the intermolecular N−O distance in these is between 2.726 and 2.887 Å.[77] Only one of them, a uranyl complex, has the coordinated aminoxyl bonding to the metal cation in a side-on fashion[78] (Figure 7) while the other examples are O-coordinated.

Dimer **10** is bound by nearly 17 kcal/mol relative to two aminoxyls in our calculation; it emerges as the most stable aminoxyl dimer. That degree of stabilization is high for N···H−O hydrogen bonded species, and merits further discussion.

There has been some mention of neutral radical-molecule hydrogen bonds in the literature, mostly with a neutral proton donating solvent.[79−81] The cyclic double hydrogen bonding pattern has been noticed for some simple radical-molecule complexes in a study by Hernández-Soto et al.[81] In that study, just as for our dimer **10**, the unpaired electron of the radical-molecule complexes is not directly involved in the hydrogen bond, but resides in an orbital perpendicular to the plane of the hydrogen bonds. Furthermore, they found that the two hydrogen-bonds do not contribute to the total binding energy in a simple additive fashion. This cooperative phenomenon is common and exists for hydrogen-bonded systems of neutral molecules. The strength of the n $\rightarrow\sigma^*$ donor−acceptor interaction was attributed to the unusually strong binding in those radical−molecule complexes.

In order to better understand the hydrogen-bond strength in dimer **10**, we looked at $H_2NO\cdots H_2O$ and $H_2NO\cdots NH_3$ model

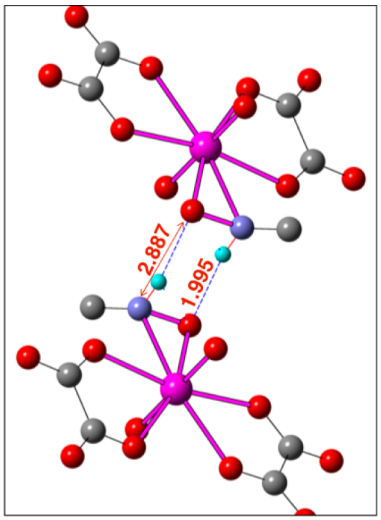

Figure 7. A piece of the crystal structure of a U-coordinated RHNO complex where a dimer **10**-like structure forms. The oxygen (red), nitrogen (light blue), hydrogen (cyan), and uranium (magenta) atoms are represented as spheres. In the zoom-in figure, some atoms are omitted for clarity. The full structure is in the SI.

systems, to see the behavior of the component hydrogen-bond moieties. The starting geometries were chosen to mimic the analogous hydrogen bonds in dimer **10**, meaning that the O···H···N distances and angle are kept the same as in dimer **10**. Also, during geometry optimization, the O−H−N distances and angle are fixed. The constrained but otherwise optimized structures and binding energies (in kcal/mol) are shown in Figure 8b,c. The binding energies of these complexes are substantial.

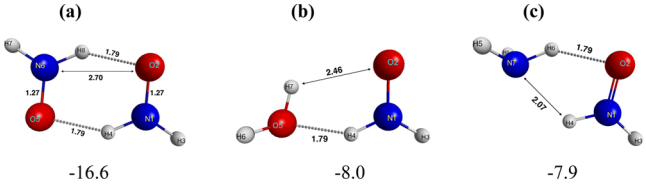

Figure 8. (a) optimized dimer **10**; (b) $H_2NO\cdots H_2O$ optimized with constraints specified in text; (c) constrained optimization of an $H_2NO\cdots NH_3$ complex.

If the non-hydrogen-bonded H atom of each H_2NO is simply removed, we reach an HNO dimer, a complex of two singlet molecules. The initial geometry of $(HNO)_2$, based on H removal from **10**, is high in energy, but if it is allowed to readjust, it comes to the structure shown in Figure 9a. This is bound relative to two separated HNO molecules by only −4.3 kcal/mol. The intermolecular O···H distance of 2.33 Å is long for a hydrogen bond.

Another model might be a dimer of hydroxylamine, H_2NOH. In this molecule the NH_2 group is not coplanar with the OH, and one gets a very different hydrogen bonding pattern, quite strong, shown in Figure 9b.

A reviewer has helpfully inquired about possible hydrogen bonded analogues to **10** for RR'NO dimers, R, R' = H, or alkyl. We have not yet explored these computationally. We expect such bonding for R═H, and the uranyl complex structure cited above shows it. The possibility of C−H···O hydrogen bonding in the case where there is an α-hydrogen on an alkyl group is

DOI: 10.1021/acs.jpca.5b12674
J. Phys. Chem. A 2016, 120, 1283−1296

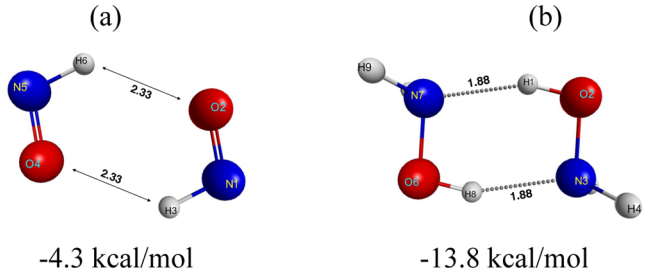

Figure 9. Calculated structures for (a) HNO dimer; (b) hydroxylamine dimer$(H_2NOH)_2$. Each N in hydroxylamine bears two hydrogens; they appear superimposed in the view shown. The binding energies shown below the figures are relative to their respective separated monomers.

possible, and is related to a reaction channel of such aminoxyls to hydroxylamine and a nitrone.[51]

As we will see in the next section, the various isomers of the aminoxyl dimer should rearrange without much activation energy to the hydrogen-bonded minimum **10**. So one might observe it in a cold matrix. But there is another interesting potential fate of this dimer, which we will discuss in a subsequent section.

2.7. Other Transition Metal Complexes of H_2NO. Since all the dimer **10**-like structures found turned out to be coordinated to a metal, we did a CSD structure search for one or two H_2NO units coordinated to a metal. All the metal complexes found with two H_2NO (a total of 12) are vanadium complexes with seven-coordination in a pentagonal bipyramidal structure. The popularity of these is probably due to the rising interest in the insulin-mimetic property of vanadium complexes.[82] Six metal complexes structures were found with only one coordinated H_2NO,[83] three of which are molybdenum complexes, including the one in Figure 6. In the literature these metal complexes are all referred to as metal hydroxylamido complexes. One reason for this nomenclature may lie in how these complexes are prepared. For example, In the case of the molybdenum complex, it is the hydroxylamine solution in ether that was added to a solution of $[Mo(NO)(Tp^{Me2})I_2]\bullet C_6H_5CH_3$ in butyl alcohol. For various vanadium complexes, solid $H_2NOH\bullet HCl$ was added to the reaction solution.[84] In these metal complexes, the N−O bond length of the (H_2NO) ligand is in the range of 1.37 Å −1.42 Å, lying in between H_2NO radical (1.26 Å) and H_2NO^- (1.44 Å) at MP2/cc-pVTZ level. We think this indicates loss of radical character, but one would need to look at other properties to draw a definite conclusion.

We reserve judgment on just what is the form of coordinated H_2NO in these complexes, given the usual crystallographic uncertainties in locating hydrogens.

2.8. Pyramidalization and Alternative Structures. The second-order mixing, of π into π^* on the same radical (through their interaction with the π and π^* orbitals of the other radical), is how the NO bonds elongate (as we see in dimers **5a** and **6a**). Other changes in molecular geometry may accompany the interaction of two aminoxyls: variable pyramidalization at N atoms, and slight elongation of N−H bonds, for instance. We wanted to see the energetic consequences of each geometrical deformation, so we considered the following sequence of steps, in each case applied to two monomer units separated and oriented as they are in the optimized dimer.

Step 1: Bring two rigid H_2NO monomers together and elongate the intramolecular N−O and N−H bond lengths so that the intermolecular separations agree with the optimized $(H_2NO)_2$ structures yet keep the monomers planar.

Step 2: Pyramidalize at both nitrogen atoms, reaching the optimized dimer geometry.

The outcome (Table 3) is fairly clear: most of the energy of interaction is set in the first step, the interaction of planar monomer radicals. Where the interaction of two aminoxyls is repulsive, pyramidalization at N then brings about significant stabilization. This may be sufficient to overcome the first step destabilization (**6a**, **7a**, **8a**), or it may not (**5a**). Where there is stabilization in the first step, pyramidalization is ineffective. We found that elongation of NO bond lengths is relatively unimportant in dimerization.

Table 3. Binding Energy Relative to Two Separated Monomers in kcal/mol[a]s

	Step1	Step2
5a	43.1	16.8
6a	2.9	−9.8
7a	12.7	−1.0
8a	9.0	−5.0
9a	−10.5	−11.9
10	−16.6	−16.6

[a]Step 1 brings together two monomers at the optimal dimer intermolecular separation and adjusts molecular bond lengths to agree with the final optimized $(H_2NO)_2$, while keeping the monomers planar. In Step 2, pyramidalization at both nitrogen centers is allowed, which results in the fully optimized dimer structure.

The positive (repulsive) energy of interaction of unperturbed H_2NO radicals for **5a** is impressively large. In an MO perspective, we see here a large four-electron destabilization in the π orbitals, which are more localized on O than on N. Alternatively, the strong repulsion can be attributed to the lone pairs of O atoms that are close to the σ bond.

2.9. Diradical Character. Now that we have examined each structure in some detail, we bring together the energies and intermolecular separations of the dimers in Table 3. We also want to describe the diradical character of all species, in a way to see how far or how little they have been transformed from two noninteracting aminoxyls.

There are a number of ways to define radical character. We chose one based on a natural orbital analysis carried out on the system, after which one looks at the occupation number of the lowest formally unoccupied natural orbital. The diradical character is taken as that population, called n_L.[85] An open-shell singlet, having n_L of ∼1, places two electrons of opposite spins in two degenerate orbitals. At the other extreme, a diradical character of zero corresponds to a closed-shell singlet. In the $(H_2NO)_2$ system, dimer **5a** is close to a closed-shell singlet, whereas the singlet state of dimer **10** is an open-shell one. As shown in Table 4 below, the other dimers all have substantial diradical character, implying that a single configurational description of their electronic structure is not adequate. So it is good that we used a multireference method in our calculations.

Table 4 tabulates the calculated binding energies of dimers (defined here as ΔE for the reaction $2R \rightarrow R_2$) in descending order. Interestingly, the closest intermolecular separation and the diradical characters both get larger in this order. The latter

DOI: 10.1021/acs.jpca.5b12674
J. Phys. Chem. A 2016, 120, 1283−1296

Table 4. $(H_2NO)_2$ Dimers in Descending Order of Binding Energy, for Each the Closest Intermolecular Distances (O−O, N−N, or N−O), Diradical Character (See Text for Definition) and Triplet−Singlet Gap Given the Same Geometry

dimer	binding energy (kcal/mol)	intermolecular separation (Å)	diradical character (# electrons, n_L)	T−S gap (eV)
5a	16.8	1.53 (O−O)	0.108	4.29
7a	−1.0	1.91 (N−O)	0.266	2.04
8a	−5.0	2.51 (O−O)	0.355	1.72
		2.09 (N−N)		
6a	−9.8	2.16 (N−N)	0.450	1.02
9a	−11.9	2.37 (N−O)	0.486	0.97
10	−16.6	2.70 (N−O)	0.914	0.02

trend (correlation of diradical character with separation), of course will continue. However, at some point, the energetic stabilization that we see, the other part of the correlation, must disappear.

2.10. A Generalized Bonding Model for $(H_2NO)_2$. In frontier molecular orbital thinking, the orbitals that are interacting as the dimer structures form are the singly occupied (SO) π^* MO, except for dimer **10**. In the 2-electron-2-orbital (2,2) active space, given the same SOMOs, we can construct a prototypical orbital interaction picture: the larger the overlap between these two orbitals, the greater the level splitting, the lower the energy of the closed-shell singlet, and the smaller the diradical character expected. This indeed is the case for two classical σ radicals, such as $\bullet CH_3$, interacting. The energy−diradical character correlation shown in Table 3 clearly does *not* follow this expectation; something else is going on here. Participation of other, lower-lying orbitals, is suggested. Let us examine this.

Figure 10 shows a schematic interaction of the π and π^* orbitals of two interacting aminoxyls. We are now in a four-orbital-six-electron space. As the two monomer radicals approach each other, in zeroth order the degenerate pairs of orbitals interact. In that interaction there is a net repulsive four-electron component, arising from the interaction between the π orbitals, and a 2-electron attractive interaction between the π^* ones. The overall picture allows us to see how there can be a net rise in energy (the repulsive interaction dominating) even as there is bond formation. As we see in dimer **5a**. In other words, the optimal geometry is a fine balance between repulsive π orbital interaction and attractive π^* orbital interaction, usually resulting in an intermolecular separation with only modest binding energy (e.g., **9a**) and preserving substantial diradical characters.

The argument we have given is a molecular orbital one. The balance of stabilization and destabilization that obtains in bond formation can be seen in a quite equivalent VB way: The dimers are formed in a conceptual sequence of energy-lowering bond formation following a localization (this takes energy) of the three-electron π systems into a localized lone pair π and a radical (also π) on N or O.

2.11. Transition States for Dimer Interconversion. Now that we have examined the local minimum energy structures of $(H_2NO)_2$, and have seen that the energy of dimer formation in all is less than 16 kcal/mol, let us turn our attention to transition states relating them. To anticipate a result obtained with much effort—for the entire set of dimers, the barriers separating less from more stable local minima are predicted to be smaller than 4 kcal/mol.

One way to think about the weakly bound dimers of H_2NO we have located, given the model of the previous section, is to classify them based on how many lobes of the SOMO π^* orbital overlap effectively. Class I includes dimer **5a**, **6a**, and **7a**, with only one lobe of the π^* orbital from each H_2NO being in contact; class II includes dimers **8a** and **9a** with both lobes of the π^* orbital being in contact. Dimer **10** belongs to a separate class III, with no direct contact between the two π^* orbitals, but strong hydrogen bonding. Transition from class I to class II, in principle, can be achieved by either rotation or sliding (Figure 11). There is always some overlap between the SOMOs of the

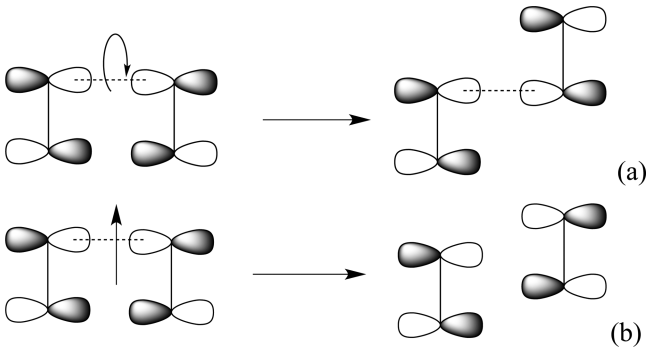

Figure 11. Plausible transition from class I to class II dimers (a) by rotation (b) sliding.

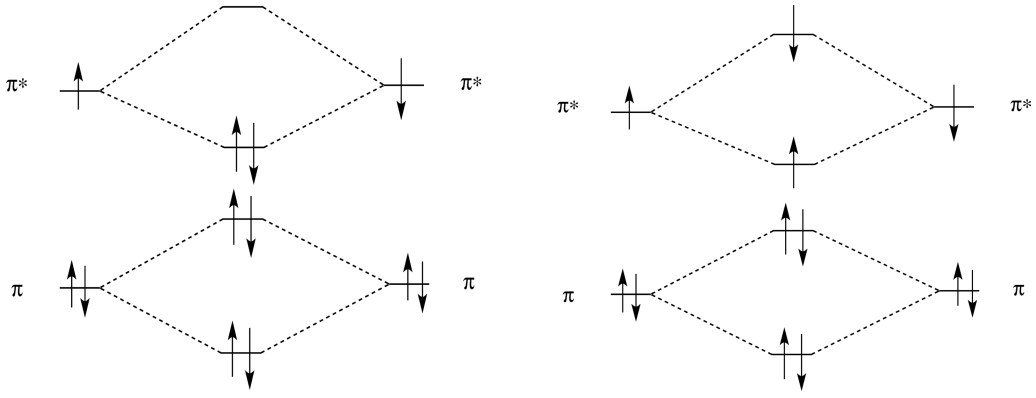

Figure 10. Schematic orbital interaction diagram between the π and π^* orbitals of H_2NO. Left: closed-shell singlet configuration; right: open-shell singlet configuration.

DOI: 10.1021/acs.jpca.5b12674
J. Phys. Chem. A 2016, 120, 1283−1296

two radicals during the entire process of rotation (Figure 11a). However, the overlap diminishes, even passes potentially through zero, as one radical slides relative to the other (Figure 11b). Hence, as far as the two-electron stabilizing interaction we outlined above goes, rotation is likely to be an energetically more favorable reaction coordinate for dimers to move from one minimum to another than sliding.

Focusing on rotation of one dimer relative to another, three routes could be envisaged, as shown in Figure 12 for specific

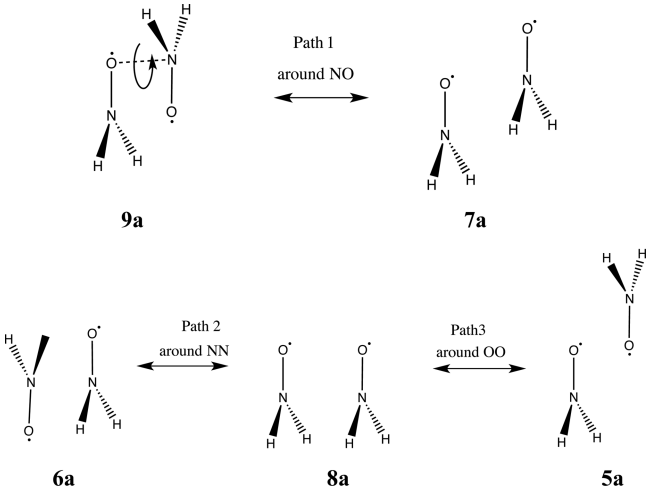

Figure 12. Possible rotational pathways among $(H_2NO)_2$.

structures. However, since most $(H_2NO)_2$ structures are weakly bound, obviously dissociation followed by dimerization to a more stable configuration is a competing path that needs to be considered for any transformation.

The complexity of the reaction pathways interrelating the dimers becomes apparent in considering the relatively unstable (+16.8 kcal/mol) local minimum of dimer **5a**. If we take O−O as a reaction coordinate, we find a tiny <1 kcal/mol barrier to dissociation to two aminoxyls (see SI Figure S7)

Moreover, there are two reaction trajectories with essentially no additional activation that lead from **5a** to more stable structures. In one, a slight O−O stretching is followed by a dissociation-recombination process and then a rotation around N−N, moving some 27 kcal/mol downhill to dimer **6b**. It takes little motion to go over from **5a** to **8a**, gaining 22 kcal/mol of stabilization.

Furthermore, there is a pathway from **5a** to the global minimum dimer, hydrogen-bonded structure **10**. The pathway is shown in Figure 13; a rotation around the O−O bond is followed by a rotation around local NO axes. Our calculated barrier for this process is only ∼2.1 kcal/mol.

In a similar way, we looked at the potential surface interrelating **6a**, **7a**, **8a**, **9a**, and **10**. Though each of these is a local minimum, the barriers separating each from a nearby more stable structure are calculated to not be larger than 4 kcal/mol. If these numbers prove reliable, then the best one might hope for is to isolate the structures in a very cold matrix. However, if one were to heat up the matrix just a little, any isomer would rearrange to **10**.

Examination of the rotational transition pathways mentioned in Figure 12 reveals that the rotational barriers are all rather small, comparable with the dissociation barriers. Hence these two motions are easily coupled with each other; for example, during the stretching of the O−O bond of **5a**, a rotation around

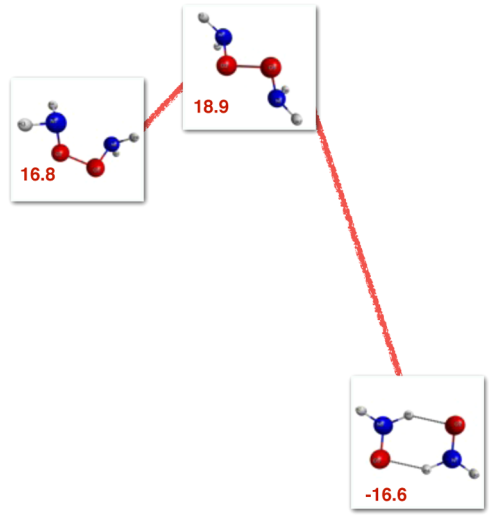

Figure 13. One reaction pathway connecting **5a** and **10**. The energies of the reactant, transition state and product are all relative to the isolated H_2NO, in kcal/mol.

N−N leads to **6b**. There are also complex reaction trajectories leading to multiple products, for instance, from **7a** to **9a** and **10**, or from **8a** to **9a** and **10**.

Two geometries that appear close to each other are the ring, **9a**, and the hydrogen-bonded dimer, **10**. One only needs a rotation of both monomers about their own molecular N−O bonds (a process different than the rotations described in Figure 12) to interconvert the two. It takes little activation energy to accomplish this, ∼ 1 kcal/mol (Figure 14).

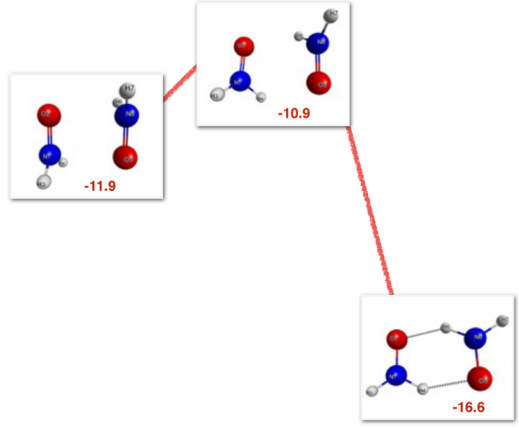

Figure 14. Rotational pathway between dimer **9a** and **10**. The energies of the reactant, transition state and product are all relative to the isolated H_2NO, in kcal/mol.

2.12. Potential Reactions of the Most Stable Dimer.

What about possible escape routes for dimer **10**? One reaction pathway that one can envisage is a double hydrogen transfer from $(H_2NO)_2$ to $(HNOH)_2$ (Figure 15). This latter dimer, which is also stabilized by hydrogen bonding, is ∼17 kcal/mol uphill from **10**. So this is not a productive pathway, even if no activation were needed (we calculate one of 21 kcal/mol).

A different escape route could be to a nitroso compound (HNO) and hydroxylamine (H_2NOH), both of which are closed-shell molecules. This is a seemingly simple process, which transfers a hydrogen atom from one H_2NO to the other

DOI: 10.1021/acs.jpca.5b12674
J. Phys. Chem. A 2016, 120, 1283−1296

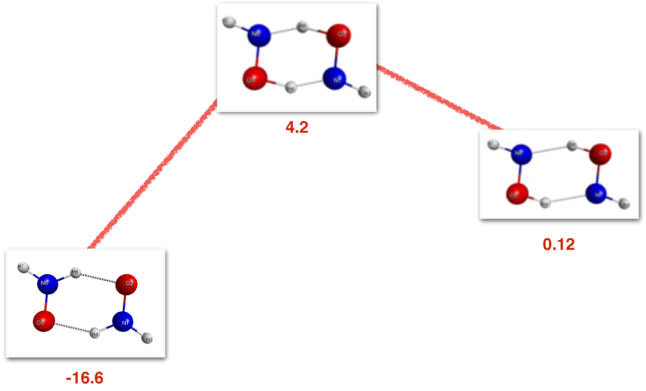

Figure 15. Double hydrogen transfer from dimer **10** to a $(HNOH)_2$ structure. The energies of the reactant, transition state, and product are all relative to the isolated H_2NO, in kcal/mol.

following a least linear motion within the molecular plane, as shown schematically in Figure 16a. However, such a planar

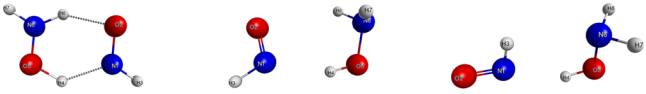

Figure 16. (a) Planar HNO···H_2NOH complex I. This structure is ~25 kcal/mol higher than the hydrogen-bonded H_2NO structure, dimer **10**. (b) Complex II. (c) Complex III.

nitroso + hydroxylamine structure is calculated as highly unstable (in fact it emerges as a second-order saddle point on the MP2 surface), ~ 15.4 kcal/mol less stable than separated HNO and H_2NOH, and 8.5 kcal/mol higher than the two separated H_2NO radicals, our energy reference.

The optimal structure of H_2NOH is not planar. Also, there are two minimum-energy structures of the HNO···H_2NOH complex, II and III (Figure 16b,c), with a transition barrier ~9 kcal/mol between them. The most stable form, complex III, is stable by 14 kcal/mol relative to the two separated H_2NO radicals. However, to get from the planar complex I to more stable forms, II or III, is very difficult.

The problem is the correlation of orbital occupation in such a process. If we consider the closed-shell singlet state of dimer **10**—effectively, a mixture of $(H_2NO···H_2NO)$ and $(H_2NO^+···H_2NO^-)$ valence structures in the same geometry as dimer **10**—such a state is 10.8 kcal/mol higher than its open-shell singlet counterpart, despite the presence of both electrostatic attraction and hydrogen-bonding. In the planar H_2NOH, there are two electrons in the π^* orbitals (and two in the π orbitals); such a 4-electron-2-orbital situation is destabilizing. To transform from the planar to nonplanar hydroxylamine optimal structure, a large orbital rearrangement would be required, suggesting a very large barrier. Hence this reaction channel is unlikely for the hydrogen bonded H_2NO dimer.

2.13. Aggregation of Hydrogen-Bonded H_2NO Dimers. Organomagnetic materials based on neutral radicals such as aminoxyls are of much interest, and among these, hydrogen-bonded assemblies are not rare.[86] Our primary intent is not to design new molecular magnets based on H_2NO, but we mention two interesting hypothetical tetrameric structures, which can be considered as extensions of the hydrogen bonding patterns of **10**. Structure **11** (Figure 17a) is planar, an oligomer on the way to a hypothetical one-dimensional polymeric supramolecular H_2NO system. This planar structure has four unpaired electrons, each residing in one of the four molecular orbitals resulting from the combination of the four π^* orbitals of H_2NO monomer. The binding energy of this tetramer is ~50.1 kcal/mol, essentially tripling the binding energy of dimer **10**. This association energy appears to be cumulative. This is an interesting way to stabilize an H_2NO unit.

The other tetramer, **12**, can be viewed alternatively as two hydrogen-bonded dimer **10** structures stacking, or probably better, as two four-membered ring **9a** structures hydrogen-bonded. In this structure, the binding energy (−55.4 kcal/mol) is roughly the sum of 2×dimer **9a** binding energy and 2×dimer **10** binding energy (−57.1 kcal/mol). These two bonding patterns have not been observed to our knowledge. Another piece of evidence that structure **12** is better viewed as two **9a** structures that are hydrogen-bonded, comes from the occupation numbers of the natural orbitals in the active space (we use this as a measure of diradical character), which are quite similar to that in dimer **9a**, rather than **10**. Structure **11**, on the other hand, remains roughly as a pair of open-shell singlets. The ground state of **12** is a singlet, with a triplet lying only 27.1 kcal/mol higher, and the quintet 61.0 kcal/mol higher still.

3. CONCLUSION

In this study, we have examined in detail the complex potential energy surface for dimerizing the parent aminoxyl, H_2NO. The monomer is nearly planar, with its unpaired electron in a π^* orbital distributed nearly equally over N and O.

One could imagine dimers of H_2NO in which N−N, N−O, or O−O single bonds are formed, as well as more unusual four-

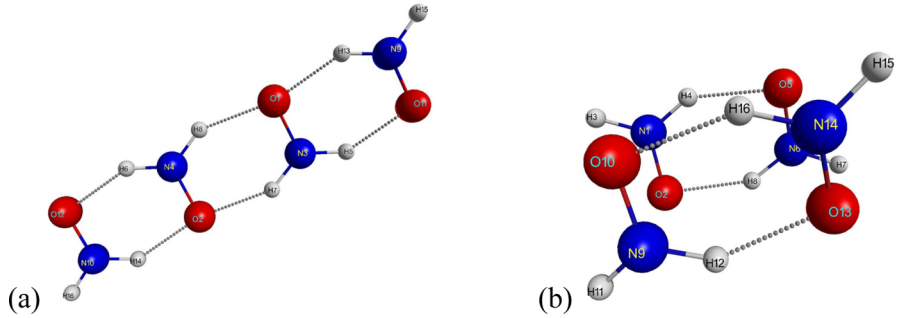

11 **12**

Figure 17. (a) planar $(H_2NO)_4$ (b) stacking $(H_2NO)_4$.

DOI: 10.1021/acs.jpca.5b12674
J. Phys. Chem. A 2016, 120, 1283−1296

membered ring structures, unsymmetrical 4-center-6-electron systems. In fact, all of these are realized as local minima. The O−O bonded species is quite unstable, and the other minima 1 to 12 kcal/mol stabilized relative to two isolated radicals.

The dimers are very different from normal radical dimers, showing much weaker bond formation. We suggest the following bonding perspective: When two π radical monomers approach each other face-on, a compromise between repulsive π (4-electron) and attractive π^* orbital interactions is made. The situation is quite different from the usually very exothermic dimerization of σ radicals. In fact, out of the six minimum-energy structures we located on the $(H_2NO)_2$ surface, only the highest minimum, **5a**, forms a σ O−O bond. Yet that structure has almost no barrier to dissociation. All the other five minimum-energy structures are weakly bound complexes retaining substantial diradical character.

A relationship is made with other 4-center 6-electron systems. So dimer **9a**, the "head-to-tail" rectangular arrangement, is iso(valence)electronic with the known Jahn−Teller distorted S_4^{2-}. Its characteristic rectangular or rhomboid geometry is observed in several larger aminoxyl crystal structures.

The most stable $(H_2NO)_2$ turns out to be a cyclic hydrogen-bonded dimer structure in which the SOMO is perpendicular to the cyclic plane and not involved in the hydrogen bond. One should be able to observe this dimer in matrix isolation studies.

The potential energy surface of $(H_2NO)_2$ is quite complex, characterized by small barriers (<4 kcal/mol) between local minima. Dissociative and rotational trajectories of low energy are characteristic of the interconversions. We return to the consistent bonding picture of the weakly bound dimers; in them one finds a balance of repulsive four-electron interaction between the π electrons of the interacting units, and an attractive two-electron interaction of the singly occupied radical π^* levels.

4. COMPUTATIONAL METHODOLOGY

The GAMESS electronic structure suite[87,88] was used in all our calculations. Local minima and transition states were first optimized with B3LYP/cc-pVTZ and confirmed by Hessian calculations. B3LYP structures and orbitals are used as starting guessed structures and orbitals for multireference perturbation theory (MRMP) calculations. It is worth mentioning that a multireference level of theory is crucial here. The global minimum energy structure predicted by MRMP (dimer **10**) is a true diradical, which B3LYP completely fails to find, and in fact, identified a transition state.

In terms of the size of the active space, we have explored two options. One is the minimal active space, (2,2), that is, two electrons in what in the aminoxyl case turn out to be two π^* SOMOs. The other one is a larger active space, (6,4), that is, six electrons in four orbitals, two of which are the π^* SOMOs and the other two are the corresponding π orbitals. By comparing the optimized geometries and binding energies, we found that both choices of active space gave similar structures and binding energies.

It is important to always examine the orbitals in the active space after optimization, in particular when there is a significant change in bonding. For example, we initially located two more local minimum-energy dimer structures that form essentially a covalent O−O bond, using the (2,2) active space. Despite having no imaginary frequencies, these two structures do not retain the appropriate orbitals in the active space. Furthermore, they turned out not to be stationary points using the (6,4) active space.

Due to the numerical nature of the MRMP Hessian calculations, small imaginary frequencies occur sometimes. We have encountered one such case (dimer **7a**) and using the larger active space did not seem to affect the outcome. In general a larger active space, just like using a larger basis set, is always better. However, since we would like to explore reaction pathways and transition states using the same level of theory, we decided to use the smaller active space, (2,2), as a compromise between accuracy and efficiency.

For dimer dissociation and rotational processes, we chose, for each dimer structure, a specific reaction coordinate and performed constrained optimization along it to see whether a local energy maximum exists. Once a maximum was found, we then fully relax the structures before and after that local maximum to see if they fall into different minimum-energy structures. For reactions of one dimer a transition state search was performed on a guessed structure along the least linear motion following the relevant mode with imaginary frequency. Once confirmed by the Hessian calculation as a first-order saddle point, intrinsic reaction coordinate (IRC) calculations were carried out to find the "reactant" and "product" connected by the reaction path.

To estimate the triplet-singlet gap, we calculated the triplet state energies using the optimized singlet structures of $(H_2NO)_2$. To assess the stability of those hypothetical triplet states, we optimized these structures using the same level of theory, MRMP(2,2)/cc-pVTZ, for the lowest triplet state.

■ ASSOCIATED CONTENT

Supporting Information

The Supporting Information is available free of charge on the ACS Publications website at DOI: 10.1021/acs.jpca.5b12674.

$(H_2NO)_2$ potential energy surface (PES) dependence on level of theory; defining degree of pyramidalization; crystal structures of a selection of dimeric R_2NO molecules; understanding **8a** and **9a**; $(H_2NO)_2$ PES for dimer **5a** (PDF)

■ AUTHOR INFORMATION

Corresponding Author

*E-mail: rh34@cornell.edu.

Notes

The authors declare no competing financial interest.

■ ACKNOWLEDGMENTS

P.X. and R.H. gratefully acknowledge the support from Energy Frontier Research in Extreme Environments (EFree) Center, an Energy Frontier Research Center funded by the U.S. Department of Energy, Office of Science under Award Number DESC0001057. Support was also received from the National Science Foundation through Grant CHE1305872. We would like to thank Tao Zeng, Bo Chen, and Miklos Kertesz for valuable advice and comments. P.X. would like to thank S. MacMillan for helping with CSD structure search.

■ REFERENCES

(1) Neiman, M. B.; Rozantzev, E. G.; Mamedova, Y. U. G. Free Radical Reactions Involving No Unpaired Electrons. *Nature* **1962**, *196*, 472−474.

DOI: 10.1021/acs.jpca.5b12674
J. Phys. Chem. A 2016, 120, 1283−1296

(2) Rozantsev, E. G.; Sholle, V. D. Synthesis and Reactions of Stable Nitroxyl Radicals II. Reactions1. *Synthesis* **1971**, *1971*, 401−414.
(3) Stone, T. J.; Buckman, T.; Nordio, P. L.; McConnell, H. M. Spin-Labeled Biomolecules. *Proc. Natl. Acad. Sci. U. S. A.* **1965**, *54*, 1010−1017.
(4) Keana, J. F. W. Newer Aspects of the Synthesis and Chemistry of Nitroxide Spin Labels. *Chem. Rev.* **1978**, *78*, 37−64.
(5) Fischer, H. The Persistent Radical Effect: A Principle for Selective Radical Reactions and Living Radical Polymerizations. *Chem. Rev.* **2001**, *101*, 3581−3610.
(6) Tamura, M.; Nakazawa, Y.; Shiomi, D.; Nozawa, K.; Hosokoshi, Y.; Ishikawa, M.; Takahashi, M.; Kinoshita, M. Bulk Ferromagnetism in the β-Phase Crystal of the P-Nitrophenyl Nitronyl Nitroxide Radical. *Chem. Phys. Lett.* **1991**, *186*, 401−404.
(7) Aminoxyl Radicals. In *IUPAC Compendium of Chemical Terminology*; IUPAC: Durham, NC, 2014.
(8) Berliner, J. L. History of the Use of Nitroxides (Aminoxyl Radicals) in Biochemistry: Past, Present and Future of Spin Label and Probe Method. In *Nitroxides - Theory, Experiment and Applications*; Kokorin, A., Ed.; InTech: Rijeka, Croatia, 2012.
(9) Adams, J. Q.; Nicksic, S. W.; Thomas, J. R. Paramagnetic Resonance of Alkyl Nitroxides. *J. Chem. Phys.* **1966**, *45*, 654.
(10) Davies, P. B.; Dransfeld, P.; Temps, F.; Wagner, H. G. Detection of the NH_2O Radical by Far Infrared LMR. *J. Chem. Phys.* **1984**, *81*.376310.1063/1.448175
(11) Gutch, C. J. W.; Waters, W. A. The Electron Spin Resonance Spectra of Some Hydroxylamine Free Radicals. *J. Chem. Soc.* **1965**, 751−755.
(12) Chawla, O. P.; Fessenden, R. W. Electron Spin Resonance and Pulse Radiolysis Studies of Some Reactions of Peroxysulfate ($SO_4^{\bullet -}$). *J. Phys. Chem.* **1975**, *79*, 2693−2700.
(13) Jinguji, M.; Imamura, T.; Murai, H.; Obi, K. ESR Study of the Dihydronitroxide (H_2NO) Radical in a Xenon Matrix at Low Temperature. *Chem. Phys. Lett.* **1981**, *84*, 335−338.
(14) Mikami, H.; Saito, S.; Yamamoto, S. The Microwave Spectrum of the Dihydronitrosyl Radical, H_2NO ($^2B_1$). *J. Chem. Phys.* **1991**, *94*, 3415.
(15) Salotto, A. W.; Burnelle, L. Ab Initio Calculation of H_2NO Geometry and Hyperfine Splittings. *J. Chem. Phys.* **1970**, *53*, 333.
(16) Ellinger, Y.; Subra, R.; Rassat, A.; Douady, J.; Berthier, G. Nonempirical Calculations on the Conformation and Hyperfine Structure of the Nitroxide and Ketyl Groups. Consequences of out-of-Plane Bending on Hyperfine Interactions. *J. Am. Chem. Soc.* **1975**, *97*, 476−479.
(17) Barone, V.; Cristinziano, P. L.; Lelj, F.; Pastore, A.; Russo, N. Non-Empirical and Mndo Study of the Geometry and Electronic Structure of H_2XO Radicals. *J. Mol. Struct.: THEOCHEM* **1982**, *90*, 59−64.
(18) Briere, R.; Claxton, T. A.; Ellinger, Y.; Rey, P.; Laugier, J. Orientation of Hyperfine Tensors with Respect to Chemical Bonds. Experimental and Ab Initio SCF + CI Study in the Nitroxide Series. *J. Am. Chem. Soc.* **1982**, *104*, 34−38.
(19) Barone, V.; Lelj, F.; Russo, N.; Ellinger, Y.; Subra, R. Theoretical Approach to Fluorine Substitution in X_2NO and X_2CN Free Radicals. Comparison between Ab Initio UHF and RHF + Perturbation Treatments. *Chem. Phys.* **1983**, *76*, 385−396.
(20) Pauzat, F.; Gritli, H.; Ellinger, Y.; Subra, R. Ab Initio SCF + CI Study of the Vibrational Effects in the Electron Spin Resonance Spectrum of the Simplest Nitroxide Radical: H_2NO. *J. Phys. Chem.* **1984**, *88*, 4581−4583.
(21) Kysel, O.; Mach, P.; Haring, M. Is the H_2NO. Radical Planar? Ab Initio Study with Inclusion of Electronic Correlation. *J. Mol. Struct.: THEOCHEM* **1986**, *138*, 299−304.
(22) Soto, M. R.; Page, M.; McKee, M. L. Configuration Interation Calculations of Structures, Vibrational Frequencies, and Heats of Formation for HHNO Species. *Chem. Phys. Lett.* **1991**, *187*, 335−344.
(23) Cai, Z.-L. Ab Initio Study of Three Low-Lying Electronic States of the H_2NO Radical. *Chem. Phys.* **1993**, *169*, 75−79.
(24) Komaromi, I.; Tronchet, J. M. J. The Geometry of the H_2NO Radical: Do the Quantum Mechanical Results Converge? *Chem. Phys. Lett.* **1993**, *215*, 444−450.
(25) Ricca, A.; Hanus, M.; Ellinger, Y. Conformational Dependence of Electronic Spectra in the Nitroxide Series: A MCSCF/CI Study. *Chem. Phys. Lett.* **1995**, *232*, 54−60.
(26) Ricca, A.; Weber, J.; Hanus, M.; Ellinger, Y. The Shape of the Ground and Lowest Two Excited States of H2NO. *J. Chem. Phys.* **1995**, *103*, 274.
(27) Ulich, B. L.; Hollis, J. M.; Snyder, L. E. Radio Detection of Nitroxyl (HNO): The First Interstellar NO Bond. *Astrophys. J.* **1977**, *217*, L105−L108.
(28) Hollis, J. M.;Snyder, L. E.; Ziurys, L. M.; McGonagle, D.; Haschick, A. D.; Ho, P. T. P. Interstellar HNO: Confirming the Identification. *Atoms, Ions and Molecules: New Results in Spectral Line Astrophysics*; Astronomical Society of the Pacific: San Francisco, CA, 1991; Vol. *16*, p 407.
(29) Liszt, H. S.; Turner, B. E. Microwave Detection of Interstellar NO. *Astrophys. J.* **1978**, *224*, L73−L76.
(30) McGonagle, D.; Irvine, W. M.; Minh, Y. C.; Ziurys, L. M. Detection of Nitric Oxide in the Dark Cloud L134N. *Astrophys. J.* **1990**, *359*, 121−124.
(31) Ziurys, L. M.; Apponi, A. J.; Hollis, J. M.; Snyder, L. E. Detection of Interstellar N2O: A New Molecule Containing an N-O Bond. *Astrophys. J.* **1994**, *436*, L181−L184.
(32) Olszyna, K. J.; Heicklen, J. The Reaction of Ozone with Ammonia. *Adv. Chem. Ser.* **1972**, *113*, 191−210.
(33) Kurasawa, H.; Lesclaux, R. Rate Constant for the Reaction of NH_2 with Ozone in Relation to Atmospheric Processes. *Chem. Phys. Lett.* **1980**, *72*, 437−442.
(34) Bulatov, V. P.; Buloyan, A. A.; Cheskis, S. G.; Kozliner, M. Z.; Sarkisov, O. M.; Trostin, A. I. On the Reaction of the NH_2 Radical with Ozone. *Chem. Phys. Lett.* **1980**, *74*, 288−292.
(35) Patrick, R.; Golden, D. M. Kinetics of the Reactions of Amidogen Radicals with Ozone and Molecular Oxygen. *J. Phys. Chem.* **1984**, *88*, 491−495.
(36) Yang, D. L.; Koszykowski, M. L.; Durant, J. L. The Reaction of NH_2 ($X\ ^2B_1$) with O ($X\ ^3P$): A Theoretical Study Employing Gaussian 2 Theory. *J. Chem. Phys.* **1994**, *101*, 1361.
(37) Meunier, H.; Pagsberg, P.; Sillesen, A. Kinetics and Branching Ratios of the Reactions $NH_2 + NO_2 \rightarrow N_2O + H_2O$ and $NH_2 + NO_2 \rightarrow H_2NO + NO$ Studied by Pulse Radiolysis Combined with Time-Resolved Infrared Diode Laser Spectroscopy. *Chem. Phys. Lett.* **1996**, *261*, 277−282.
(38) Peiró-García, J.; Nebot-Gil, I.; Merchán, M. An Ab Initio Study on the Mechanism of the Atmospheric Reaction $NH_2+O_3\rightarrow H_2NO +O_2$. *ChemPhysChem* **2003**, *4*, 366−372.
(39) Saito, T.; Ito, A.; Watanabe, T.; Kawakami, T.; Okumura, M.; Yamaguchi, K. Performance of the Coupled Cluster and DFT Methods for through-Space Magnetic Interactions of Nitroxide Dimer. *Chem. Phys. Lett.* **2012**, *542*, 19−25.
(40) Albright, T. A.; Burdett, J. K.; Whangbo, M.-H. Molecular Orbitals of Diatomic Molecules and Electronegativity Perturbation. In *Orbital Interactions in Chemistry*; John Wiley & Sons, Inc.: Hoboken, NJ, 2013; pp 97−122.
(41) Brown, P. J.; Capiomont, A.; Gillon, B.; Schweizer, J. Spin Densities in Free Radicals. *J. Magn. Magn. Mater.* **1979**, *14*, 289−294.
(42) Bordeaux, D.; Boucherleb, J.-X.; Delley, B.; Gillon, B.; Ressouehe, E.; Schweizer, J. Experimental and Theoretical Spin Densities in Two Alkyl Nitroxides. *Z. Naturforsch., A: Phys. Sci.* **1993**, *48*, 117−119.
(43) Gillon, B.; Becker, P.; Ellinger, Y. Theoretical Spin Density in Nitroxides. *Mol. Phys.* **1983**, *48*, 763−774.
(44) Delley, B.; Becker, P.; Gillon, B. Local Spin Density Theory of Free Radicals: Nitroxides. *J. Chem. Phys.* **1984**, *80*, 4286.
(45) Wang, J.; Smith, J. V. H. Ab Initio Study of the Spin Density of Nitroxide Radicals. *Z. Naturforsch., A: Phys. Sci.* **1993**, *48*, 109.

DOI: 10.1021/acs.jpca.5b12674
J. Phys. Chem. A 2016, 120, 1283−1296

(46) Ressouche, E.; Schweizer, J. Ab Initio Calculations Versus Polarized Neutron Diffraction for the Spin Density of Free Radicals. *Monatsh. Chem.* **2003**, *134*, 235−253.
(47) Wu, Y.-J.; Lin, M.-Y.; Hsu, S.-C.; Cheng, B.-M. Infrared Absorption Spectra of t-HNOH Radicals Generated on VUV Irradiation of NO in Solid Hydrogen. *ChemPhysChem* **2009**, *10*, 901−904.
(48) Rozantsev, E. G.; Ulrich, H. Physical Properties and Structure of Individual Radicals. In *Free Nitroxyl Radicals*; Ulrich, H., Ed.; Springer: New York, 1970; pp 119−129.
(49) Mahoney, L. R.; Mendenhall, G. D.; Ingold, K. U. Calorimetric and Equilibrium Studies on Some Stable Nitroxide and Iminoxy Radicals. Approximate Oxygen-Hydrogen Bond Dissociation Energies in Hydroxylamines and Oximes. *J. Am. Chem. Soc.* **1973**, *95*, 8610−8614.
(50) Lind, J.; Merényi, G. Kinetic and Thermodynamic Properties of the Aminoxyl ($NH_2O\bullet$) Radical. *J. Phys. Chem. A* **2006**, *110*, 192−197.
(51) Karoui, H.; Le Moigne, F.; Ouari, O.; Tordo, P. Nitroxide Radicals: Properties, Synthesis and Applications. In *Stable Radicals: Fundamentals and Applied Aspects of Odd-Electron Compounds*; Hicks, R. G., Ed.; John Wiley & Sons, Ltd: Hoboken, NJ, 2010; pp 173−229.
(52) Aurich, H. G.; Breuer, E.; Aurich, H. G.; Nielsen, A. Nitroxides. In *Nitrones, Nitronates and Nitroxides (1989)*; John Wiley & Sons, Inc.: Hoboken, NJ, 1989; pp 313−370.
(53) Linnett, J. W. *J. Am. Chem. Soc.* **1965**, *87*, 2078−2079.
(54) Linnett, J. W.; Rosenberg, R. M. Structure and Properties of Nitroso Compounds. *Tetrahedron* **1964**, *20*, 53−66.
(55) Harcourt, R. D. *Bonding in Electron-Rich Molecules: Qualitative Valence-Bond Approach via Increased-Valence Structures*; 2nd ed.; Springer International Publishing: Cham, Switzerland, 2016.
(56) Redington, R. L.; Olson, W. B.; Cross, P. C. Studies of Hydrogen Peroxide: The Infrared Spectrum and the Internal Rotation Problem. *J. Chem. Phys.* **1962**, *36*, 1311.
(57) Tsuboi, M.; Overend, J. Amino Wagging and Inversion in Hydrazines: ^{R}R Branch of the Antisymmetric Wagging Band of NH_2NH_2. *J. Mol. Spectrosc.* **1974**, *52*, 256−268.
(58) Gurvich, L. V.; Veyts, I. V.; Alcock, C. B. *Thermodynamic Properties of Individual Substances*; 4th ed.; Hemisphere Publishing Corp.: New York, 1989.
(59) Mealli, C.; Ienco, A.; Messaoudi, A.; Poduska, A.; Hoffmann, R. Parallel Disulfido Bridges in Bi- and Poly-Nuclear Transition Metal Compounds: Bonding Flexibility Induced by Redox Chemistry. *Inorg. Chim. Acta* **2008**, *361*, 3631−3637.
(60) Mealli, C.; Ienco, A.; Poduska, A.; Hoffmann, R. S_4^{2-} Rings, Disulfides, and Sulfides in Transition-Metal Complexes: The Subtle Interplay of Oxidation and Structure. *Angew. Chem., Int. Ed.* **2008**, *47*, 2864−2868.
(61) Poduska, A.; Hoffmann, R.; Ienco, A.; Mealli, C. Half-Bonds" in an Unusual Coordinated S_4^{2-} Rectangle. *Chem. - Asian J.* **2009**, *4*, 302−313.
(62) Del Sesto, R. E.; Miller, J. S.; Lafuente, P.; Novoa, J. J. Exceptionally Long (≥2.9 Å) CC Bonding Interactions in π-$[TCNE]_2^{2-}$ Dimers: Two-Electron Four-Center Cation-Mediated CC Bonding Interactions Involving π^* Electrons. *Chem. - Eur. J.* **2002**, *8*, 4894−4908.
(63) Casado, J.; Burrezo, P. M.; Ramírez, F. J.; Navarrete, J. T. L.; Lapidus, S. H.; Stephens, P. W.; Vo, H.-L.; Miller, J. S.; Mota, F.; Novoa, J. J. Evidence for Multicenter Bonding in Dianionic Tetracyanoethylene Dimers by Raman Spectroscopy. *Angew. Chem.* **2013**, *125*, 6549−6553.
(64) Cui, Z.; Lischka, H.; Mueller, T.; Plasser, F.; Kertesz, M. Study of the Diradicaloid Character in a Prototypical Pancake-Bonded Dimer: The Stacked Tetracyanoethylene (TCNE) Anion Dimer and the Neutral K_2TCNE_2 Complex. *ChemPhysChem* **2014**, *15*, 165−176.
(65) Preuss, K. E. Pancake Bonds: π-Stacked Dimers of Organic and Light-Atom Radicals. *Polyhedron* **2014**, *79*, 1−15.
(66) Howie, R. A.; Glasser, L. S. D.; Moser, W. Nitrosodisulphonates. Part II. Crystal Structure of the Orange-Brown Triclinic Modification of Fremy's Salt (Potassium Nitrosodisulphonate). *J. Chem. Soc. A* **1968**, 3043−3047.
(67) Capiomont, A.; Chion, B.; Lajzérowicz, J. Affinement de La Structure Du Radical Nitroxyde Dimerisé: bicyclo[3,3,1]nonanone-3 Aza-9 Oxyle-9. *Acta Crystallogr., Sect. B: Struct. Crystallogr. Cryst. Chem.* **1971**, *27*, 322−326.
(68) Kurokawa, G.; Ishida, T.; Nogami, T. Remarkably Strong Intermolecular Antiferromagnetic Couplings in the Crystal of Biphenyl-3,5-Diyl Bis(tert-Butyl Nitroxide). *Chem. Phys. Lett.* **2004**, *392*, 74−79.
(69) Allen, F. H. The Cambridge Structural Database: A Quarter of a Million Crystal Structures and Rising. *Acta Crystallogr., Sect. B: Struct. Sci.* **2002**, *58*, 380−388.
(70) CSD Refcodes for the 17 "head-to-Tail" Dimer 9a-like Structures: APUYEP, AZOMAD, BUZWOZ01, CYNOAZ10, CYNOAZ11, ELUREJ, ELUREJ01, ELUROT, MISYAP, PIXBUV, ROSHIQ, SAQLUR, UHOLAE, UHOLEI, KULSAN, KULSER, and KULSER01.
(71) In search for dimer **9a**-like structures, we set the intermolecular N···O distances to be in the range of 1.7−2.7 Å. If larger distances are allowed, more structures will be found. Miklos Kertesz kindly suggested five structures with intermolecular N···O distances longer than 2.7 Å. Some of these do not strictly have a rectangular shape, presumably due to the large R group. These structures have the following CSD refcodes: BASKAI, DIGJEK, EDIZIZ, LEBKOT, and RERXES03.
(72) Miklos Kertesz showed us an informative graph in which all the 17 structures in the CSD have an N−O···N(O) angle differing by no more than 4° from 90°.
(73) Danen, W. C.; Newkirk, D. D. Nitrogen-Centered Free Radicals. IX. The Ease of Formation of Thionitroxide Radicals. *J. Am. Chem. Soc.* **1976**, *98*, 516−520.
(74) Maillard, B.; Ingold, K. U. Kinetic Applications of Electron Paramagnetic Resonance Spectroscopy. XXII. Dialkylaminothiyl Radicals. *J. Am. Chem. Soc.* **1976**, *98*, 520−523.
(75) Hicks, R. G. What's New in Stable Radical Chemistry? *Org. Biomol. Chem.* **2006**, *5*, 1321−1338.
(76) Włodarczyk, A. J.; Romańczyk, P. P.; Lubera, T.; Nitek, W. Synthesis, Characterisation and Crystal Structure of Hydroxylamido-κ2N,O(iodo)[tris(3,5-Dimethylpyrazol-1-yl)borato]-nitrosylmolybdenum(II). *Inorg. Chim. Acta* **2011**, *367*, 217−221.
(77) CSD Refcodes for dimer **10**-like structures: FOPJID, IXENEE, IXENII, JAGWUJ,QECKAK, QUXXOX, UMIREN, UMIRIR, XINFOQ, XOBVIU, and YOLBUX.
(78) Beirakhov, A. G.; Orlova, I. M.; Il'in, E. G.; Gorbunova, Y. E.; Mikhailov, Y. N. Uranyl Complexes with Acetophenone Oxime. *Russ. J. Inorg. Chem.* **2007**, *52*, 34−41.
(79) Franchi, P.; Lucarini, M.; Pedrielli, P.; Pedulli, G. F. Nitroxide Radicals as Hydrogen Bonding Acceptors. An Infrared and EPR Study. *ChemPhysChem* **2002**, *3*, 789−793.
(80) Nakajima, S.; Kato, E.; Minatozaki, M.; Nishide, H. A Supramolecular Polymer of Nitroxide Radicals via Hydrogen Bonding. *Macromol. Symp.* **2011**, *304*, 1−7.
(81) Hernández-Soto, H.; Weinhold, F.; Francisco, J. S. Radical Hydrogen Bonding: Origin of Stability of Radical-Molecule Complexes. *J. Chem. Phys.* **2007**, *127*, 164102.
(82) Keramidas, A. D.; Miller, S. M.; Anderson, O. P.; Crans, D. C. Vanadium(V) Hydroxylamido Complexes: Solid State and Solution Properties1. *J. Am. Chem. Soc.* **1997**, *119*, 8901−8915.
(83) CSD Refcodes for structures with One H_2NO Coordinated to a Metal: AQHPRV, COZJOQ, SAKSOM, SAKSOM10, UMEVUE, YINBUS.
(84) Wieghardt, K.; Quilitzsch, U.; Nuber, B.; Weiss, J. Dipicolinato-(hydroxylamido-O,N) (nitrosyl)aquavanadate—A Nitrosyl Complex of Vanadium with "side On" Coordinated Hydroxylamine. *Angew. Chem., Int. Ed. Engl.* **1978**, *17*, 351−352.
(85) Flynn, C. R.; Michl, J. pi., .pi.-Biradicaloid Hydrocarbons. O-Xylylene. Photochemical Preparation from 1,4-Dihydrophthalazine in

DOI: 10.1021/acs.jpca.5b12674
J. Phys. Chem. A 2016, 120, 1283−1296

Rigid Glass, Electric Spectroscopy, and Calculations. *J. Am. Chem. Soc.* **1974**, *96*, 3280−3288.
(86) Lahti, P. M. Structure−Property Relationships for Metal-Free Organic Magnetic Materials. In *Advances in Physical Organic Chemistry*; Richard, J. P., Ed.; Academic Press: London, 2011; Vol. 45, pp 93−169.
(87) Schmidt, M. W.; Baldridge, K. K.; Boatz, J. A.; Elbert, S. T.; Gordon, M. S.; Jensen, J. H.; Koseki, S.; Matsunaga, N.; Nguyen, K. A.; et al. General Atomic and Molecular Electronic Structure System. *J. Comput. Chem.* **1993**, *14*, 1347−1363.
(88) Gordon, M. S.; Schmidt, M. W. Advances in Electronic Structure Theory: GAMESS a Decade Later. In *Theory and Appications of Computational Chemistry: The First Forty Years*; Elsevier B.V.: Amsterdam, 2005; pp 1167−1189.

DOI: 10.1021/acs.jpca.5b12674
J. Phys. Chem. A 2016, 120, 1283−1296